Interface Charge Density Matching as Driving Force for New Mesostructured Oxovanadium Phosphates with Hexagonal Structure, $[CTA]_xVOPO_4 \cdot zH_2O$

Jamal El Haskouri, Manuel Roca, Saúl Cabrera, Jaime Alamo, Aurelio Beltrán-Porter, Daniel Beltrán-Porter, M. Dolores Marcos,* and Pedro Amorós*

Institut de Ciència dels Materials de la Universitat de València (ICMUV), Dr. Moliner no. 50, 46100-Burjassot, València, Spain

Received August 5, 1998. Revised Manuscript Received March 8, 1999

Hexagonal mesostructured mixed-valence oxovanadium phosphates $[CTA]_xVOPO_4 \cdot zH_2O$, in short ICMUV-2, have been synthesized through a S^+I^- cooperative mechanism using cationic surfactant (cetyltrimethylammonium, CTAB) rodlike micelles as a template. On the lines of the hypothesis that the driving force leading to the formation of mesostructured solids is the charge density matching at the interface between the supramolecular−organic and supramolecular−inorganic moieties, the self-assembling process between CTA^+ micelles and $VOPO_4^{q-}$ planar anions can be thought of as consequence of the adequate adjustment of the metal mean oxidation state. X-ray powder diffraction and TEM techniques show that the solids consist of hexagonal arrays of mesopores filled with surfactant, whereas spectroscopic results allow us to propose an oxovanadium phosphate bond topology similar to that observed in the $Na_xVOPO_4 \cdot nH_2O$ layered derivatives. The thermal behavior of the mesostructured materials has also been investigated, given that both the easy elimination of CTA^+ species and their V:P = 1:1 molar ratio make ICMUV-2 solids adequate pyrolytic precursors of the $(VO)_2P_2O_7$ catalyst.

Introduction

Vanadium phosphorus oxides constitute an interesting and complex system with catalytic relevance. Thus, $(VO)_2P_2O_7$ has been recognized as the active phase in catalysis for high selectivity commercial production of maleic anhydride, an important raw material used in polyester resin production from C4 hydrocarbons.[1,2] This conversion is the only heterogeneously catalyzed alkane-selective oxidation reaction in commercial use.[3] In turn, $(VO)_2P_2O_7$ can be obtained by pyrolysis of several of the many crystalline phases characterized in the V−P−O system.[4] The structural diversity in this system, which expands from 3-D networks to layered and microporous materials,[5−8] is actually a remarkable feature. Moreover, the chemistry of oxovanadium phosphates has recently aroused a renewed interest because of the possibility of incorporating into the resulting frameworks organic or inorganic species, which frequently are referred to as "templates" or "structural directing agents".[9]

The current trend in the synthesis of new open structures is clearly the search for pore systems in the range of mesopores. There can be no doubt that Mobil research reported in 1992, describing the synthesis of mesoporous silica (MCM-41) by using micelles and aggregates of long-chain surfactants as supramolecular templates, constituted a major step forward in this field of activity.[10] The supramolecular templating method was quickly adapted to the preparation of a large number of non-silica-based mesostructured/mesoporous materials (due to their potential applicability as catalysts, molecular sieves or host matrixes).[11−15] Whereas such a method "opens new horizons for the design of porous materials",[15] it must be recognized that the state of the art relating to the synthesis of these materials shows still a great number of unanswered questions, mainly as a result of a lack of detailed mechanistic

* Authors to whom correspondence should be addressed: P.A., e-mail pedro.amoros@uv.es; and M.D.M., e-mail loles.marcos@uv.es.

(1) Centi, G.; Trifiro, F.; Ebner, J. R.; Franchetti, V. M. *Chem. Rev.* **1988**, *88*, 55.
(2) Centi, G. *Catal. Today* **1993**, *16*, 5.
(3) Coulston, G. W.; Bare, S. R.; Kung, H.; Birkeland, K.; Bethke, G. K.; Harlow, R.; Herron, N.; Lee, P. L. *Science* **1997**, *275*, 191.
(4) Amorós, P.; Ibáñez, R.; Beltrán, A.; Beltrán, D.; Fuertes, A.; Gómez, P.; Hernandez, E.; Rodriguez, J. *Chem. Mater.* **1991**, *3*, 407.
(5) Beltrán, D.; Beltrán, A.; Amorós, P.; Ibáñez, R.; Martínez, E.; Le Bail, A.; Ferey, G.; Villeneuve, G. *Eur. J. Solid State Inorg. Chem.* **1991**, *28*, 131.
(6) Zubieta, J. *Comments Inorg. Chem.*, **1992**, *39*, 569.
(7) Khan, M. I.; Meyer, L. M.; Haushalter, R. C.; Schweitzer, A. L.; Zubieta, J.; Dye, J. L. *Chem. Mater.* **1996**, *8*, 43.
(8) Roca, M.; Marcos, M. D.; Amorós, P.; Alamo, J.; Beltrán, A.; Beltrán, D. *Inorg. Chem.* **1997**, *36*, 3414.
(9) Davis, M. E.; Lobo, R. F. *Chem. Mater.* **1992**, *4*, 756.
(10) (a) Kresge, C. T.; Leonowicz, M. E.; Roth, W. J.; Vartuli, J. C.; Beck, J. S. *Nature* **1992**, *359*, 710. (b) Beck, J. S.; Vartuli, J. C.; Roth, W. J.; Leonowicz, M. E.; Kresge, C. T.; Schmitt, K. D.; Schlenker, J. L. *J. Am. Chem. Soc.* **1992**, *114*, 10834.
(11) Huo, Q.; Margolese, D. I.; Cielsa, U.; Demuth, D. G.; Feng, P.; Gier, T. E.; Sieger, P.; Firouzi, A.; Chmelka, B. F.; Schüth, F.; Stucky, G. D. *Chem. Mater.* **1994**, *6*, 1176.
(12) Behrens, P. *Angew. Chem., Int. Ed. Engl.* **1996**, *35*, 515.
(13) Attard, G. S.; Göltner, C. G.; Corker, J. M.; Henke, S.; Templer, R. H. A. *Angew. Chem., Int. Ed. Engl.* **1997**, *36*, 1315.
(14) Corma, A. *Chem. Rev.* **1997**, *97*, 2373.
(15) Sayari, A.; Liu, P. *Microporous Mater.* **1997**, *12*, 149.

10.1021/cm9805572 CCC: $18.00
Published on Web 05/07/1999

information.[16] Although the initial approaches considered that the obtaining of these type of materials goes through a crystal liquid templating state,[10,17] it seems now that the entire process is more appropriately described—in the case of low surfactant concentration—on the basis of the cooperative organization of both organic and inorganic moieties.[18] If so, the key for the formation of mesostructured solids should be the charge density matching at the organic−inorganic interface.[18,19]

By assuming such a "surface charge density matching" model, Stucky et al. demonstrated that the strategy of synthesis used for silica derivatives could be extended to the preparation of other mesoporous materials,[18] although the required procedural variables may vary markedly from one to another system. In practice, most of the work developed mainly on silica-based mesoporous solids has been focused on the influence of the surfactant characteristics on the resulting materials,[20−22] but the possible influence of the inorganic counterpart in the synthesis conditions has gone rather unnoticed. However, if the matching of charge density at the surfactant−inorganic interface governs the mesostructure assembly process, not only the nature of the surfactant molecules but also the hydrolysis and condensation reactions concerning the inorganic species in solution must acquire an important role in the process. In this context, it should be noted that contrary to the easy hydrolysis and condensation reactions of silicium cations in aqueous media,[23] many metals show a shorter progression of their hydrolytic processes.[24] Hence, strong limiting problems affecting charge density matching at the interface might appear.

With reference to the V−P−O system, as far as we are aware, there are two previous reports concerning mesostructured materials.[25,26] Thus, by using the hydrothermal technique, Iwamoto and col.[25] synthesized for the first time V−P−O mesostructured materials having a hexagonal array of the pores filled with surfactants. These materials have a V:P molar ratio of 2:1, and their walls were considered as probably consisting of an "amorphous phase of vanadium oxide and phosphorus oxide".[25] On the other hand, Doi and Miyake[26] reported also on the synthesis of one hexagonal mesostructured V−P−O compound having the same V:P = 2:1 molar ratio. Instead of the one-step procedure used by Iwamoto et al.,[25] Doi and Miyake developed a two-step method[26] similar to that of FSM-16 silicates.[14,15] In this case, a lamellar V−P−O compound containing surfactant (whose V:P molar ratio was 1:0.85) was obtained by intercalation of the surfactant in $VO(HPO_4)\cdot 0.5H_2O$, and this intermediate material was then subjected to a hydrothermal treatment to give the hexagonal (V:P = 2:1) mesostructured compound. As far as the V:P molar ratio in these hexagonal mesostructured materials is 2:1, they should be very likely inadequate as precursors of mesostructured catalytic phases (given that the active phase has the V:P = 1:1 molar ratio).

In this work, we report the low-temperature preparation and characterization of new hexagonal mesostructured oxovanadium phosphates, $[CTA]_xVOPO_4\cdot zH_2O$ (CTA= cetyltrimethylammonium)—hereafter, ICMUV-2—having the V:P= 1:1 molar ratio.

Table 1. Selected Synthetic and Compositional Parameters and X-ray Data for ICMUV-2 Solids: $[CTA]_x[(V^{IV}O)_y(V^{V}O)_{1-y}PO_4]\cdot zH_2O$

sample	V(IV) solution (%)	V(IV) y	CTA^+ x	water z	d_{100} (Å)	a^a (Å)
1	35	0.20	0.20	2.01	37.09	42.6(6)
2	45	0.25	0.24	1.80	39.07	45.1(6)
3	50	0.33	0.33	1.50	38.38	44.8(5)
4	55	0.36	0.37	1.41	38.38	45.3(6)
5	58	0.49	0.49	1.16	38.05	44.7(5)
6	60	0.54	0.53	1.01	38.71	45.6(5)
7	65	0.58	0.57	0.95	37.09	44.0(6)
8	75	0.61	0.59	0.76	40.50	45.6(6)
9	85	0.61	0.60	0.65	38.71	45.5(6)
10[b]	75	0.52	0.53	1.00	39.06	46.1(3)

[a] Calculated cell parameter taking into account a hexagonal cell similar to that described for MCM-41 silicas and using the well resolved peaks unambiguously indexed in the hexagonal cell: (100) for samples 1 and 2; (100), (110) and (200) for samples 3, 4, and 5; (100), (110), (200) and (210) for samples 6 and 7; (100) and (200) for samples 8 and 9. [b] Sample prepared under soft-hydrothermal conditions: 120 °C during 72 h.

Experimental Section

Synthesis of $[CTA]_xVOPO_4\cdot zH_2O$. Mesostructured mixed-valence oxovanadium phosphates with different V(IV):V(V) content (ICMUV-2 solids) have been synthesized using CTAB (cetyltrimethylammonium bromide) as a surfactant-directing agent in water. Constant $V:H_3PO_4$:CTAB:water molar ratios equal to 1:5:0.1:150 were always used in the starting mixtures, in which the V(IV):V(V) content can be adjusted in a continuous way by addition of varying amounts of H_2O_2 (in the absence of surfactant).

In a typical sample preparation, an aqueous suspension (50 mL) containing V metal (0.226 g, 4.44 mmol), V_2O_5 (1.617 g, 8.88 mmol), and 7.6 mL of 85% H_3PO_4 was refluxed until complete dissolution (pH = 1.2), leading to a dark blue solution (characteristic of VO^{2+} cations). Different amounts of H_2O_2 were then added to adjust the desired V(IV):V(V) ratio. Subsequently, a solution (10 mL) of CTAB (0.81 g, 2.22 mmol) was added while stirring at room temperature, and homogenized during 1 h. The resulting green solids were filtered off, washed repeatedly with water, and air-dried. The main analytical data, including the V(IV):V(V) molar ratios in the mother solution and in the final materials, as well as the surfactant (x) and water (z) contents of selected mesostructured solids, have been summarized in Table 1.

In some cases, a hydrothermal posttreatment was used to improve crystallinity. The homogenized $V:H_3PO_4$:CTAB:water suspensions were placed in a Teflon digesting bomb (23 mL), filled to 80% of its volume, and statically heated at an external temperature of 120 °C under autogenous pressure for different periods of time.

Analysis. Vanadium and phosphorus contents were determined, after dissolution of the solids in boiling concentrated nitric acid, by atomic absorption spectrometry (Perkin-Elmer

(16) Francis, R. J.; O'Hare, D. *J. Chem. Soc., Dalton Trans.* **1998**, 3133.
(17) (a) Attard, G. S.; Glyde, J. C.; Göltner, C. G. *Nature* **1995**, *378*, 366. (b) Göltner, C. G.; Antonietti, M. *Adv. Mater.* **1997**, *9*, 431.
(18) Huo, Q.; Margolese, D. I.; Cielsa, U.; Feng, P.; Gier, T. E.; Sieger, P.; Leon, R.; Petroff, P. M.; Scüth, F.; Stucky, G. D. *Nature* **1994**, *368*, 317.
(19) Roca, M.; El Haskouri, J.; Cabrera, S.; Beltrán, A.; Alamo, J.; Beltrán, D.; Marcos, M. D.; Amorós, P. *J. Chem. Soc., Chem. Commun.* **1998**, 1883.
(20) Tanev, P. T.; Pinnavaia, T. J. *Science* **1995**, *267*, 865.
(21) Huo, Q.; Leon, R.; Stucky, G. D. *Science* **1995**, *268*, 1324.
(22) Manne, S.; Schäffer, T. E.; Huo, Q.; Hansma, P. K.; Morse, D. E.; Stucky, G. D.; Aksay, I. A. *Langmuir* **1997**, *13*, 6382.
(23) Brinker, C. J.; Scherer, G. W. *Sol−Gel Science. The Physics and Chemistry of Sol−Gel Processing*; Academic Press: San Diego, 1990.
(24) Baes, C. F.; Mesmer, R. E. *The Hydrolysis of Cations*; Wiley: New York, 1976.
(25) Abe, T.; Taguchi A.; Iwamoto, M. *Chem. Mater.* **1995**, *7*, 1429.
(26) Doi T.; Miyake, T. *J. Chem. Soc., Chem. Commun.* **1996**, 1635.

Zeeman 5000). Vanadium(IV) content was determined by a redox titration procedure reported elsewhere.[27] Water and surfactant contents were determined by CNH elemental and thermogravimetric analysis.

Physical Measurements. X-ray powder diffraction patterns were recorded by means of a conventional angle-scanning Seifert 3000TT diffractometer using Cu Kα radiation in steps of 0.02° (2θ) for 60 s per step.

Transmission electron micrographs (TEM) were recorded using a Phillips CM10 instrument operated at 120 kV. All the TEM samples were prepared by dispersing the powder in undecane. A drop of this suspension was placed on a TEM copper grid covered with a thin carbon film and dried in air. SEM observations were made on a Hitachi 4100FE instrument.

Infrared spectra were recorded on a FTIR Perkin-Elmer 1750 spectrophotometer using dry KBr pellets containing 2% of the sample.

Magnetic measurements were performed at 1000 G in the temperature range 2−300 K with a SQUID susceptometer Quantum Design MPMS-XL-S. Corrections for the diamagnetism of the compound were estimated using Pascal's constants.[28] ^{31}P NMR spectra were recorded at 80.962 MHz on a high-power Brucker MSL 200 spectrometer equipped with a 4.7-T superconducting magnet. The shifts of the line were referenced to 85% $H_3PO_{4(aq)}$ measured in the same probe. X-band ESR spectra were recorded on a Brucker ER 200D spectrometer.

Thermogravimetric analysis were performed with a TGA-7 Perkin-Elmer instrument under flowing nitrogen/air atmosphere at a 5 °C/min heating rate.

Results and Discussion

Synthetic Strategy. An examination of the literature, dealing with non-siliceous mesoporous/mesostructured materials,[11−15] shows that both systematic essays which find inspiration in the MCM-41 preparation method (trial and error) and strategies based on rationalizing hypothesis have proved to be useful synthetic tools. At this point, our synthesis method, which assumes the "surface charge density matching" Stucky's model,[18] includes also a simple idea: the resulting framework in the final material would be influenced by the nature of the inorganic aggregates present in the mother solution (an idea whose usefulness has been already proven in the case of other related open-framework materials).[8,29] In practice, lacking appropriate thermodynamic (and kinetic) data, only a good knowledge of the solution chemistry of the precursor species in standard conditions might constitute a tentative guide in the search for rational synthesis designs. We therefore have considered two orientative basic tools to approach the preparative chemistry of these materials: the phase diagram of the surfactant, and the knowledge of he hydrolysis and condensation reactions of the inorganic species in solution.

With regard to the organic component, according to its phase diagram, the surfactant concentration we have used is intermediate between cmc1 and cmc2. Hence, nonorganized micellar aggregates must be the dominant species in aqueous media.[30] Then, precipitation of hexagonal mesophases cannot be expected as resulting from a liquid crystal templating mechanism but through a cooperative organization of the inorganic and organic species. On the other hand, in that concerning to the hydrophilic inorganic species, the syntheses described here have been carried out at very low pH values. Under these conditions, the majority oxovanadium species in solution are the isolated aqua cations. In the presence of oxophosphorus anions ($H_2PO_4^-$ at the working pH), their successive hydrolysis and condensation reactions can give rise, as we have previously shown,[8,29] to the formation of $[VOPO_4]_m^{n-}$ two-dimensional anions. In turn, these anions can be thought of as precursors of lamellar and microporous phosphates in which the (OV)-di-μ(O,O′)PO_4-(VO) fragment is recognizable as the main structural unit.[8,29] The high hydrophilic character of the $[VOPO_4]_m^{n-}$ anions could modify the hydration degree around the different species in solution and, when water is scarce in the mixture, it could cause a decrease in the hydration degree around the CTA^+ species (i.e., it could "formally" increase the surfactant local concentration), this favors the formation of rodlike micelles. Hence, among the previously proposed mechanisms,[10,18] a S^+I^- cooperative mechanism between $[VOPO_4]_m^{n-}$ anions and CTA^+ cylindrical micelles seems to be the most adequate to explain the formation of the title compounds. The $[VOPO_4]_m^{n-}$ fragments are flexible enough to twist around the large cationic supramolecular templates, and we can benefit from the adaptability of these inorganic fragments to construct mesostructured oxovanadium phosphates. Accordingly, the charge density matching at the surfactant−inorganic interface would govern the assembly process, and, consequently, the type of mesostructure generated. Thus, it seems clear the importance of the charge modulation in the supramolecular aggregates to obtain a proper matching between the inorganic and organic species. Until now, most of the efforts had been directed to control the charge density of the surfactant aggregates: changing the hydrophobic chain-length,[31] using organic expansors,[32] or using different surfactant types.[20−22] In this case, we have focused our attention on the inorganic counterpart: as there are two easily accessible oxidation states for the vanadium atoms, the modification of the V(IV):V(V) molar ratio in the $(VOPO_4)^{n-}{}_m$ moieties can modulate the charge at the inorganic surface in a range comprised between $q = -1$ and $q = 0$ elemental charges per vanadium atom.

A simple picture of the CTA^+ micelles is one in which the shape is approximately rodlike with the hydrocarbon chains confined to the core, shielded from the aqueous solvent, and the polar headgroups oriented to the interface. In this case, we can consider that the most probable surfactant aggregation is the hexagonal close packing of the charged headgroups at the micelle surface. By taking into account the van der Waals radius of the of CTA^+ headgroups (4.5 Å) and the diameter of the rodlike micelles (37.5 Å),[33] it is possible to calculate its surface charge density, $q^+ = 0.014$

(27) Casañ, N.; Amorós, P.; Ibáñez, R.; Martínez, E.; Beltrán, A.; Beltrán, D. *J. Inclusion Phenom.* **1988**, *6*, 193.
(28) Boudreaux, E. A.; Mulay, L. N. *Theory and Applications of Molecular Paramagnetism*; John Wiley & Sons: New York, 1976; p 491.
(29) Roca, M.; Marcos, M. D.; Amorós, P.; Beltrán, A.; Edwards A. J.; Beltrán, D. *Inorg. Chem.* **1996**, *35*, 5613.
(30) Laughlin, R. G. *The Aqueous Phase Behavior of Surfactants*; Academic Press: London, 1994.
(31) Ulagappan, N.; Rao, C. N. R. *J. Chem. Soc., Chem. Commun.* **1966**, 2759.
(32) Beck, J. S. U.S. Patent 5,057,296, 1991.
(33) Warr, G. G.; Sen, R.; Evans, D. F.; Trend, J. E. *J. Phys. Chem.* **1988**, *92*, 774.

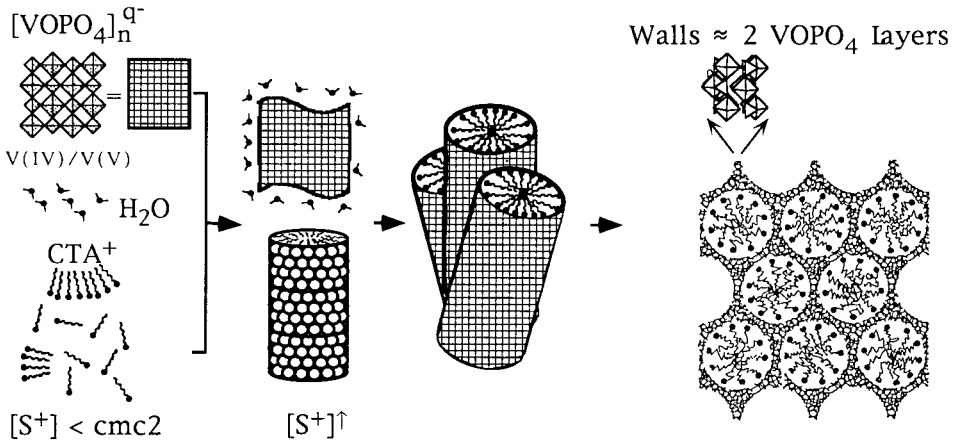

Figure 1. Schematic representation of the S^+I^- cooperative formation mechanism for ICMUV-2 mesostructured oxovanadium phosphates.

elementary charges/Å^2. From this value, and assuming that the bond topology in the inorganic network likely is similar to that adopted in the mixed-valence derivatives $Na_xVOPO_4 \cdot nH_2O$[8,27,34] and $VOPO_4 \cdot 2H_2O$[8] (see below), we have calculated that the best V(IV):V(V) molar ratio to achieve an optimum charge matching between the inorganic and organic supramolecular species in the final $VOPO_4$/surfactant composite material should be 0.54:0.46. However, the micelles are not rigid entities, and it may be expected that the charge matching be fulfilled not only for a single value but for a range. This "matching interval" would extend only slightly toward higher proportions of V(IV), as far as it would imply more compacted micelles. On the contrary, it may enlarge more broadly by lowering the V(IV):V(V) proportions, given that the micelles can easily obtain a looser packing to accommodate lower charge at the inorganic surface. In fact, we have been able to isolate mesostructured materials inside the range V(IV):V(V) = 0.2:0.8 to V(IV):V(V) = 0.6:0.4, and all the attempts to prepare mesostructured materials having higher or lower V(IV):V(V) ratios have been unsuccessful. Figure 1 shows a schematic representation of the proposed supramolecular cooperative mechanism.

Synthesis. After addition of the surfactant to the solution that contains phosphoric acid and oxovanadium cations, the respective mesostructured materials are formed in only a few minutes. We have used reaction times lower than 1 h. In fact, longer homogenization times systematically lead to mixtures of the hexagonal mesostructured material and another nonmesostructured lamellar solid, which was previously detected as an intermediate phase when V_2O_5 and phosphoric acid are treated with some reducing agent (f.e., ethanol, HI). This minority phase is really a mixed-valence oxovanadium phosphate, $(V^{V}OPO_4)_{1-x}(V^{IV}OHPO_4)_x \cdot nH_2O$, that can be isolated as single phase in conditions very similar to those here reported for our mesostructured materials, except for that of the surfactant.[35] The presence of this phase is clearly detectable by means of X-ray powder diffraction analysis.

The method we have used for the adjustment of the V(IV):V(V) ratio results is clearly advantageous (homogeneous single phase solids are obtained) when compared with other methods in which the partial reduction of cations is carried out after the addition of the surfactant or, even, once the mesostructure is formed. Examination of Table 1 shows that the stoichiometry of the resulting mesostructured material clearly depends on the V(IV):V(V) molar ratio in the starting solution. Indeed, the V(IV):V(V) molar ratio in the final solid is always lower but directly related to the one in the mother solution. The impoverishment in V(IV) is less marked when the V(IV):V(V) molar ratio in the mother solution is close to 1, whereas larger differences are observed for both higher and lower V(IV):V(V) ratios. Moreover, even when the initial CTA:(total vanadium) molar ratio has remained constant, it is the CTA:V(IV) ratio which remains constant in the final solids (at a value close to one). Finally, another interesting correlation is that observed with respect to the water content in the final mesostructured materials: the amount of water lessens as that of V(IV) (and consequently the CTA^+ cations) increases. The correlation between the V(IV):V(V) molar ratio and the water content is in good accordance with previous studies on mixed-valence lamellar oxovanadium phosphates containing Na^+ cations between layers.[27]

On the other hand, all the solids have been investigated, with negative results, for the presence of Br^- anions. Hence, the partial oxidation of V(IV) in the mother solution, which seems to act as "motor" for the formation of mesostructured materials, induces a defect of negative charge in the inorganic framework which must be balanced by lowering the CTA^+ density inside the composite material. We have experimentally found the upper and lower limits for the V(IV):V(V) molar ratio in the mesostructured materials, and, consequently, for the amount of CTA^+. Neither longer heating times (or soft-hydrothermal treatments) nor the addition of progressively smaller amounts of H_2O_2 has allowed us to obtain any solid having more than 0.61 V(IV) cations per V atom. In a similar way, all the attempts to isolate single phases containing less than 0.2 V(IV) cations per V atom, by addition of an excess of oxidant, have been unsuccessful.

When the as synthesized mesostructured solids are treated under soft-hydrothermal conditions, solids with lower CTA^+/V molar ratio can be obtained as consequence of a partial oxidation of V(IV). From a structural

(34) Wang, S. L.; Kang, H. Y.; Cheng, C. Y.; Lii, K. H. *Inorg. Chem.* **1991**, *30*, 3496.
(35) Amorós, P. Tesis de Licenciatura, Universitat de València, 1986.

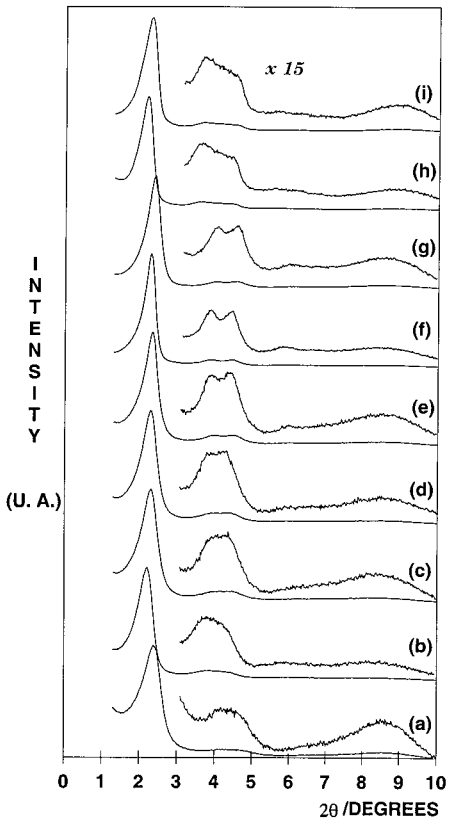

Figure 2. X-ray powder diffraction patterns of ICMUV-2 mesostructured materials: (a) sample 1 ($x = 0.20$); (b) sample 2 ($x = 0.24$); (c) sample 3 ($x = 0.33$); (d) sample 4 ($x = 0.37$); (e) sample 5 ($x = 0.49$); (f) sample 6 ($x = 0.53$); (g) sample 7 ($x = 0.57$); (h) sample 8 ($x = 0.59$); and (i) sample 9 ($x = 0.60$).

point of view, the hydrothermal treatment simply increases the crystallinity (as shown by the improvement in the resolution of the X-ray diffraction peaks). However, when the treatment is prolonged, oxidation of vanadium centers becomes important and, probably due to a reduced charge matching between inorganic moieties and micellar aggregates, a partial transformation in a new lamellar mesostructured solid occurs.

X-ray Powder Diffraction and TEM. X-ray diffraction patterns of selected ICMUV-2 solids are shown in Figure 2. As can be noted, all the samples display very similar patterns: one very intense peak at an approximately fixed d value (~38−39 Å), and some other features of lower intensity (which in some cases are resolved in four diffraction peaks). The indexation of these patterns has been done with hexagonal cells (Table 1) similar to that proposed for MCM-41 silica.[36] Despite the similarities, a clear evolution of the patterns with the V(IV) (or CTA^+) content is observed. The solids 6 and 7, with V(IV):V(V) ratios close to the one theoretically calculated for a proper matching between the $VOPO_4^{q-}$ moieties and the close-packed CTA^+ micelles (0.56:0.44), show the best resolved patterns (four peaks can be read). However, a gradual loss of crystallinity is revealed as we move away from this optimum value. Thus, in the patterns of the solids containing lower V(IV):V(V) ratios we can observe first (sample 5, 0.49:0.51; and sample 4−0.36:0.64), apart from the intense (100) low-angle reflection, only other two resolved small reflections ((110) and (200)); then (sample 3, 0.33:0.66; and sample 2, 0.25:0.75), only one broad peak is observed together with the intense (100) peak, and, finally, the pattern of he mesostructured solid containing the lowest V(IV):V(V) ratio (sample 1, 0.20−0.80) only displays clearly the (100) peak. On the other hand, the distance between the (100) and (200) reflections seemingly increases abruptly in the patterns of the solids containing high V(IV):V(V) ratios (sample 8, 0.61:0.39; and sample 9, 0.61:0.39), an unexpected result dealing with a hexagonal cell. Although the formation of an additional secondary phase might be invoked to explain this effect, we have not found evidence of it from our TEM study. Thus, to elucidate whether this effect is really due to such a new phase or it corresponds to a certain distortion of the original hexagonal cell would require a more detailed study.

As in the case of MCM-41 silicium oxide, indexation of the ICMUV-2 solid patterns gives no information about the "c" direction (all the peaks have null "l" value), which indicates that there is no long-range order along the pore direction. Thus, ICMUV-2 materials are not strictly crystalline solids. This notwithstanding, the observed diffraction peaks are consistent with a two-dimensional ordering at nanometric scale of the channel-like pores (filled by CTA^+ molecules), arranged in a hexagonal honeycomb pattern with high degree of regularity. At high 2θ angles, no discernible peak is observed in the X-ray patterns, and only a broad feature is detected between 20 and 30° (2θ). This feature is an intrinsic property of the mesostructured/mesoporous solids due to the atomic disorder in the walls, and it is also observed even for samples entirely consisting of hexagonally packed channels.[37]

Although the mesostructured ICMUV-2 materials show some differences in their respective X-ray powder diffraction patterns, all of them present practically identical TEM micrographs. Figure 3a shows a typical TEM image of ICMUV-2 (sample 6, V(IV):V(V) = 0.54:0.46). The regular hexagonal array of uniform pores is clearly recognized. TEM images reveal that all the samples display an homogeneous and regular mesopore system (filled by surfactant molecules), and they can be consequently considered as monophasic products. Figure 3b shows that ICMUV-2 particles consists of numerous "single crystal blocks" which are tilted with respect to each other in different directions.

ICMUV-2 materials have an effective pore size of 26 Å, approximately, and a wall thickness of ~13 Å (from TEM micrographs and X-ray data). The wall thickness is somewhat larger than that of MCM-41 silicas but similar to that reported for other mesostructured solids (including the previously synthesized hexagonal mesostructured V−P−O solids having a V:P = 2:1 molar ratio).[25] By taking into account the calculated wall thickness, and by assuming the hypothesis that the inorganic framework bond topology is similar to that observed in lamellar oxovanadium phosphates, the wall could be considered as constructed from two $VOPO_4$ layers (the thickness of a single $VOPO_4$ layer in crystalline lamellar phosphates is, approximately, 6−7 Å).[5]

(36) Huo, Q.; Margolese, D. I.; Stucky, G. D. *Chem. Mater.* **1996**, *8*, 1147.

(37) Schüth, F. *Ber. Bunsen-Ges. Phys. Chem.* **1995**, *99*, 1315.

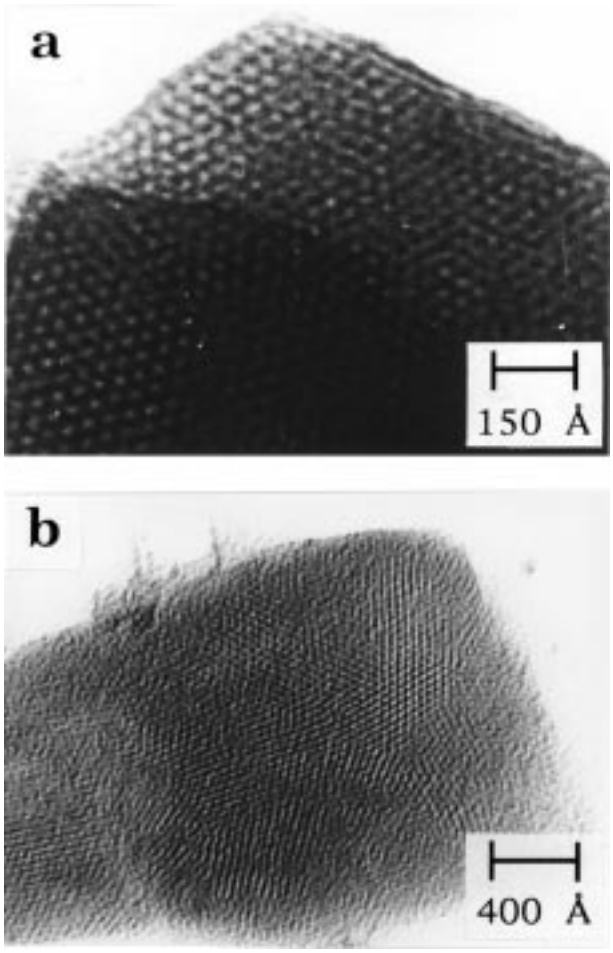

Figure 3. Characteristic TEM images of ICMUV-2 solids (sample 6): (a) high magnification image showing the ordered hexagonal pore distribution. (b) low magnification image showing the sample homogeneity.

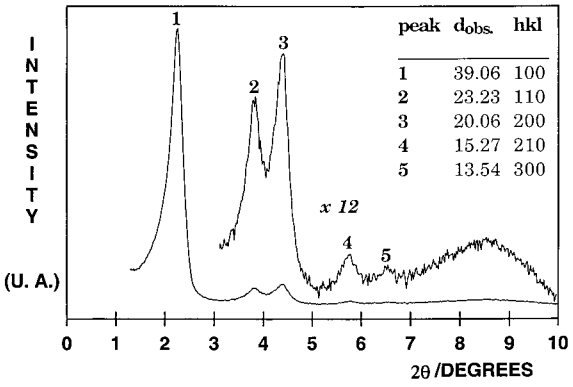

Figure 4. X-ray powder diffraction pattern and peak indexation of the hydrothermally treated ICMUV-2 sample showing a good peak resolution.

Hydrothermally treated ICMUV-2 solids display TEM images consisting of regular hexagonal mesopore distributions similar to those observed in solids obtained at room temperature. However, their X-ray powder diffraction patterns show better resolution than the corresponding prehydrothermal materials, and five reflections ((100), (110), (200), (210), and (300)) can be clearly distinguished (Figure 4). Prolonged hydrothermal treatments (t > 3 days) lead to mixtures of hexagonal and lamellar mesostructured phases.

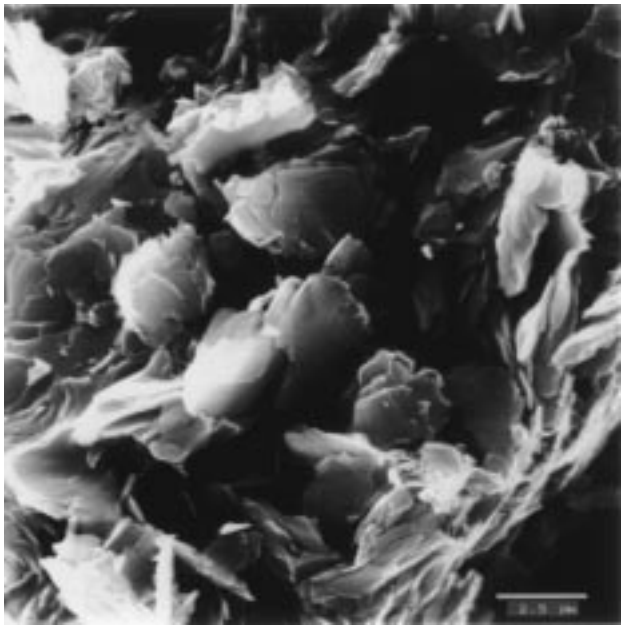

Figure 5. Typical scanning electron micrograph of ICMUV-2 solids (sample 4) in which the characteristic platelike morphology can be observed.

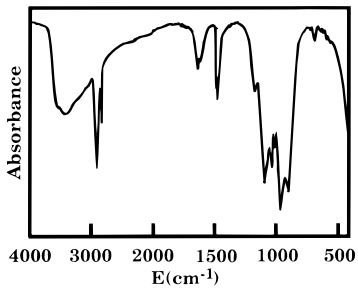

Figure 6. IR spectrum of ICMUV-2 (sample 3).

Morphological Study by SEM. All ICMUV-2 solids present similar micrometric morphological features. Thus, independently from their composition or synthetic history, our materials are built up of platelike particles with constant size and very irregular shape. Shown in Figure 5 is a typical electron micrograph of ICMUV-2 solids (sample 4).

Infrared Spectroscopy. By taking into account the noncrystalline character of the inorganic walls in the studied materials, spectroscopic techniques are the most adequate to obtain information about the atomic local distribution in the inorganic framework. Figure 6 shows an IR spectrum typical of ICMUV-2 derivatives (sample 3). Good band resolution is achieved for vibration modes both of the surfactant and $VOPO_4$ moieties. The spectrum shows sharp bands at 2920, 2845, 1460, and 1375 cm^{-1} that can be assigned to υ_{as}(C−H), υ_s(C−H), $\delta(CH_2)$, and υ(C−C) vibration modes of CTA^+ species. Bands due to the inorganic framework are located in the 800−1200 cm^{-1} range, and are similar to those appearing in the spectra of layered $Na_xVOPO_4 \cdot nH_2O$ solids.[27] Summarized in Table 2 are the IR band wavenumbers for selected ICMUV-2 materials compared with those corresponding to lamellar sodium containing oxovanadium phosphates having a similar V(IV):V(V) ratio. As the amount of V(IV) (and CTA^+) increases, a broadening of the bands of the inorganic framework is clearly ob-

Table 2. Infrared Absorption Wavenumbers (cm^{-1}) for ICMUV-2 Materials $[CTA]_x[(V^{IV}O)_y(V^{V}O)_{1-y}PO_4]\cdot zH_2O$ (Sample 1, $y = 0.20$; Sample 4, $y = 0.36$; Sample 6, $y = 0.54$) Compared with the Layered Sodium Oxovanadium Phosphates $Na_x[(V^{IV}O)_y(V^{V}O)_{1-y}PO_4]\cdot zH_2O$ ($x = 0.25, 0.37, 0.45$)

sample 1	$x = 0.25$	sample 4	$x = 0.37$	sample 6	$x = 0.45$	assignment
1173	1170	1181	1175	1180	1172	ν_{as}(PO)
1090	1087	1090	1090	1082	1080	ν_{as}(PO)
1038	1035	1041	1040	1027	1025	ν_{as}(PO)
1005	1000	1000	1000	1000	1000	ν(V=O)
970	965	965	950	975	980	ν_{s}(PO)
905	911	905	905	895	890	ν_{s}(PO)
880	872	860	875			ν_{s}(PO)

served, although no significant changes in the number or position of the bands occur. On the other hand, when comparing these IR spectra with those corresponding to previously reported hexagonal mesostructured VPO solids,[25] important differences (both in the shape and number of bands) can clearly be detected. These observations support the hypothesis that the inorganic framework in ICMUV-2 solids must present a bond topology closer to that observed in $Na_xVOPO_4\cdot nH_2O$ (hence, with short-range ordering in the walls) than to the one of the previously reported mesostructured VPO-solids.[25]

The decrease of the water content in ICMUV-2 as the V(IV) (and CTA^+) content increases is shown in Figure 7. Indeed, it is evident the opposite evolution of the δ-(OH_2) bands of water molecules and the $\delta(CH_2)$ bands of CTA^+ species. On the other hand, while the spectra of solids having high V(IV) and CTA^+ contents (V(IV): V(V) = 0.33:0.67) display a single broad band attributable to the $\delta(OH_2)$ vibration mode, the spectra of compounds with low V(IV) (and CTA^+) content display narrower and split $\delta(OH_2)$ bands. This fact, together with the two-step water evolution observed in thermogravimetric experiences, could suggest the existence of two different types of water molecules, coordinated and noncoordinated to vanadium centers, as it occurs in the case of $Na_xVOPO_4\cdot nH_2O$.[27]

Magnetic Characterization. To obtain additional information concerning the bond topology and short-range order in the disordered pore walls, we have studied the magnetic properties of ICMUV-2 oxovanadium phosphates by means of the temperature dependence of the magnetic susceptibility, ESR, and ^{31}P solid-state NMR techniques.

All samples display a very similar magnetic behavior. The susceptibility continuously decreases upon cooling, without any special features. Taking into account that no peak or broad maximum appear in the χ vs T curves, no evidence of long-range or low-dimensional magnetic interactions down to 2 K exist. Shown in Figure 8 is the temperature dependence of the reciprocal molar susceptibility of selected ICMUV-2 solids (samples 3, 6 and 8). Full susceptibility data (temperature range 2−300 K) cannot be adjusted to a Curie−Weiss law due to a small and continuous curvature of the $1/\chi$ vs T curve in all samples. The shape of these plots suggests that while at high-temperature ferromagnetic type interactions should be dominant, in the low-temperature range, the observed magnetic interactions must be due to weak antiferromagnetic interactions between V(IV) centers.

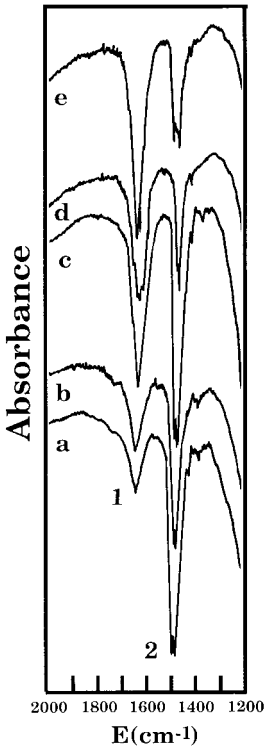

Figure 7. Evolution of the IR spectra of ICMUV-2 solids with the content of surfactant: (a) sample 9 ($x = 0.60$; $z = 0.65$); (b) sample 6 ($x = 0.53$; $z = 1.01$); (c) sample 4 ($x = 0.37$; $z = 1.41$); (d) sample 3 ($x = 0.33$; $z = 1.50$); (e) sample 1 ($x = 0.20$; $z = 2.01$). The bands marked as 1 and 2 can be assigned to δ(H−O−H) and δ(H−C−H) vibration modes of the water molecules and CTA^+ cations, respectively. The intensity of band 1 increases when intensity of band 2 decreases.

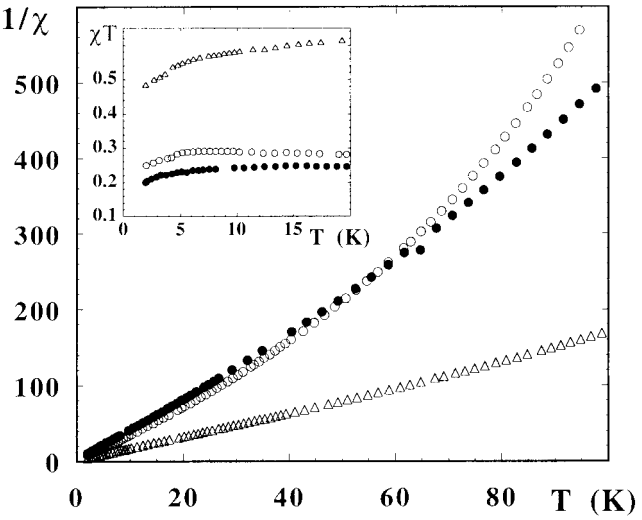

Figure 8. Thermal dependence of $1/\chi$ for selected ICMUV-2 solids: (△) sample 3 ($y = 0.33$); (●) sample 6 ($y = 0.54$); and (○) sample 8 ($y = 0.61$). In the inset, $\chi_m T$ vs T plots are represented.

The variation of the χT product with T (inset of Figure 8), which exhibits a decrease at low temperature, confirms the antiferromagnetic nature of the low-temperature interactions. On the other hand, both the fact that all ICMUV-2 materials display similar magnetic behavior and the regular variation of the curve shapes with the V(IV) content, support the existence of a random paramagnetic centers distribution in a similar

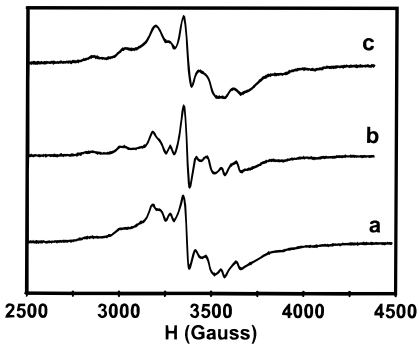

Figure 9. X-band ESR spectra of ICMUV-2 materials: (a) sample 3 ($y = 0.33$); (b) sample 6 ($y = 0.54$); and (c) sample 8 ($y = 0.61$).

inorganic lattice independently of the V(IV)/V(V) molar ratio.

All ICMUV-2 samples exhibit typical VO^{2+} ESR spectra in which the hyperfine structure due to vanadium nucleus is clearly resolved although, as expected, slightly less resolved lines appear as the V(IV) content increases (see Figure 9). Similar ESR parameters, $g_{\|} = 1.935$, $g_{\perp} = 1.985$, $A_{\|} = 198$ G, and $A_{\perp} = 75$ G, are calculated for all the samples. The fact that even at high V(IV) concentration the hyperfine structure is still observed indicates the existence of very weak dipolar and exchange interactions. Hence, the V(IV) centers must be regularly distributed throughout the inorganic network that only involves magnetically weak $V(OPO)_2V$ bridges (di-μ(O,O′)PO_4).[38] The presence of hyperfine structure in the ESR spectra of ICMUV-2 solids having high V(IV) content could be a surprising result, taking into account that the spectra of mixed-valence layered oxovanadium phosphates with a similar V(IV) content present only one isotropic signal.[27] However, this result can be understood in terms of the special structural features of the ICMUV-2 solid walls as compared with the lamellar sodium derivatives. Thus, although solids of both types must have the same bond topology inside the $VOPO_4$ inorganic framework, the $VOPO_4$ layers are very close packed (3-D framework) in the case of the sodium derivatives; in contrast, ICMUV-2 solids include only one $VOPO_4$ layer around the CTA^+ micelles. Then, in ICMUV-2 solids there will be at most two $VOPO_4$ layers as close as in the sodium derivatives (total wall thickness $\approx 2 \times$ $VOPO_4$ layers). This structural topology implies a widely separated V(IV) distribution, which will consequently result in a significant decrease of the dipolar and superexchange interactions (i.e., in the resolution of the hyperfine structure in the ESR spectra).

^{31}P solid-state NMR spectra of ICMUV-2 samples have been recorded at room temperature. In all cases, the signals appear slightly shifted from the standard ($\delta < 70$ ppm), indicating weak magnetic exchange coupling among V(IV) cations. As we have previously established, the shift of the ^{31}P NMR signals is related with the presence of finite spin density at the phosphorus nuclei, that is to say with the participation of phosphate molecular orbitals in the effective transmission of the superexchange magnetic interaction.[5,38,39] The small δ shift values, similar to those observed in oxovanadium phosphates such as $M(VOPO_4)_2 \cdot nH_2O$ ($M = Na^+$, Ca^{2+}),[38] are consistent with very weak magnetic interactions, in good accord with the susceptibility data and ESR study.

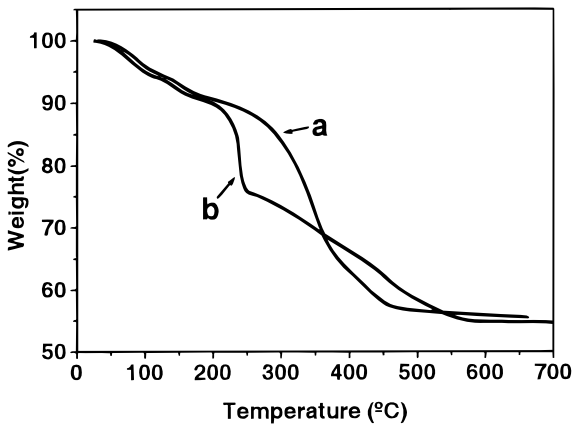

Figure 10. Typical thermal evolution of ICMUV-2 solids (sample 3) under flowing N_2 (**a** trace) and air (**b** trace) atmosphere.

In conclusion, all the available magnetic and spectroscopic data related to the pore walls are consistent with our above hypothesis concerning both the formation mechanism and bond topology of the title compounds, allowing us to discard the existence of any structural motive (f.e., dimerized or chained VO_6 octahedra) different from the $V(OPO)_2V$ chairlike bridges commonly observed in all the oxovanadium phosphates isolated at low pH conditions.[8]

Thermal Behavior. Mesostructured ICMUV-2 solids are adequate pyrolytic precursors of both the reduced $(VO)_2P_2O_7$ and oxidized $VOPO_4$ phases. There are two principal characteristics of the ICMUV-2 composite materials which make them suitable pyrolytic precursor of the VPO catalytic phases: first, its V:P = 1:1 molar ratio; second, the easy thermal evolution of the surfactant.

Two representative TGA curves (N_2 and air flowing atmosphere) of ICMUV-2 materials are shown in Figure 10 (sample 3). Like it occurs with all the remaining ICMUV-2 samples, independent of the atmosphere, template removal results in the degradation of the mesostructure. However, the fact that all our attempts to extract the template using a diversity of solvents were unsuccessful suggests that the ionic S^+I^- interactions have a significant strength. In all cases, different final compounds (as shown by their X-ray powder diffraction patterns) are obtained, depending on the working atmosphere. Whereas $(VO)_2P_2O_7$ is obtained after thermal treatment under nonoxidant (N_2) atmosphere, the β-$VOPO_4$ polymorph is the resulting solid in the case of air atmosphere. From the TGA curves, the following observations can be made: (a) no stable intermediates are evidenced in the course of the thermal evolution; (b) the weight loss of ~9% observed (N_2 or air atmosphere) in the approximately 25−200 °C temperature range can be attributed to the evolution of water

(38) Roca, M.; Amorós, P.; Cano, J.; Marcos, M. D.; Alamo, J.; Beltrán, A.; Beltrán, D. *Inorg. Chem.* **1998**, *37*, 3167.

(39) Villeneuve, G.; Suh, K. S.; Amorós, P.; Casañ-Pastor, N.; Beltrán, D. *Chem. Mater.* **1992**, *4*, 108.

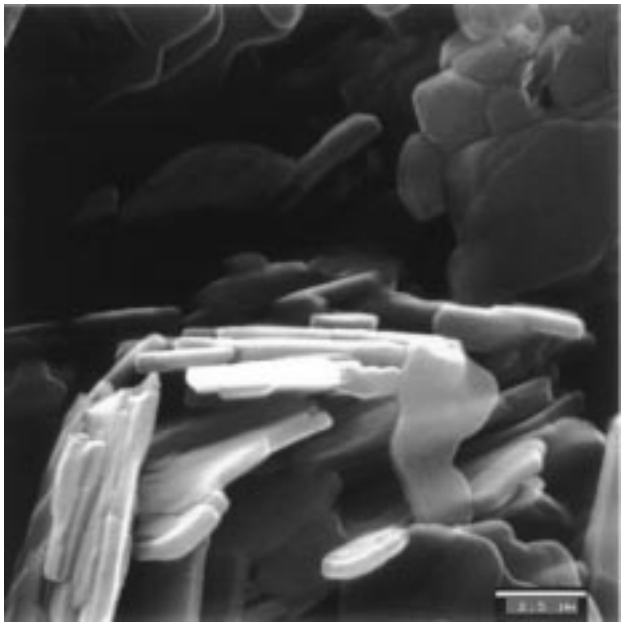

Figure 11. SEM image of β-$VOPO_4$ prepared by pyrolysis (700 °C) of ICMUV-2 (sample 3) under flowing air atmosphere.

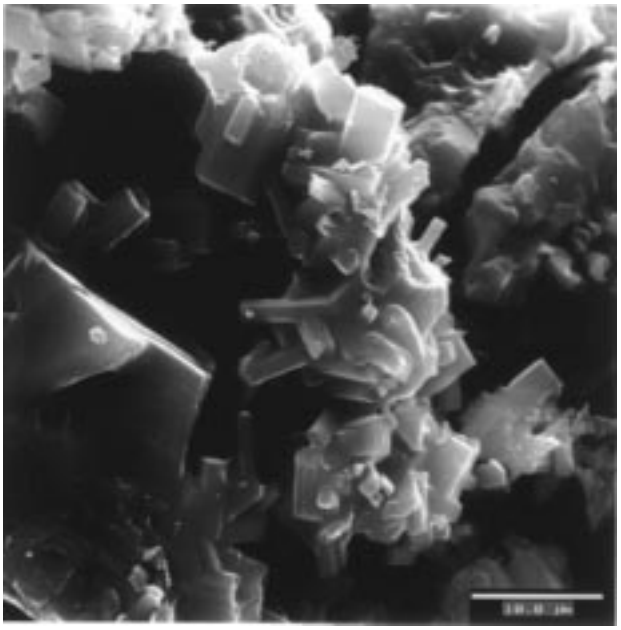

Figure 12. SEM image of $(VO)_2P_2O_7$ prepared by pyrolysis (700 °C) of ICMUV-2 (sample 3) under flowing N_2 atmosphere.

molecules; (c) water molecules evolution occurs in a two-step process, but it is difficult to unambiguously assign weight losses to individual reaction steps due to their partial overlap. However, taking into account the V(IV): V(V) molar ratio and the total water content in the solids, we can tentatively attribute the first step to the evolution of noncoordinated water molecules, and the second one to the elimination of coordinated water molecules (probably to vanadium(V) cations); (d) the total weight loss in the approximately 200−600 °C temperature range fits in well with that corresponding to the degradation of CTA^+ species (taking into account that the final solids are $(VO)_2P_2O_7$ or β-$VOPO_4$, depending on the working atmosphere). In any case, it seems evident that surfactant removal implies complex multistep processes which occur with simultaneous partial oxidation (air atmosphere) or reduction (N_2 atmosphere) of oxovanadium cations.

As far as the catalytic performance of the VPO catalysts is influenced by the particles morphology,[40,41] we have considered it convenient to undertake a preliminary microstructural characterization of the β-$VOPO_4$ and $(VO)_2P_2O_7$ solids isolated after thermal treatment of the ICMUV-2 materials. Figure 11 shows a SEM micrograph of β-$VOPO_4$. This phase mainly consists of large aggregates of crystalline platelets with an average size of 2−5 μm, and a regular thickness of 0.5 μm. On the other hand, as shown in Figure 12, particles of $(VO)_2P_2O_7$ consist of a mixture of large lamellar crystals, displaying in some cases hexagonal geometry, and small prismatic crystals in the 3−8 μm range.

(40) Igarashi, H.; Tsuji, K.; Okuhara, T.; Misono, M. *J. Phys. Chem.* **1993**, *97*, 7065.
(41) Mizuno, N.; Hatayama, H.; Misono, M. *Chem. Mater.* **1997**, *9*, 2697.

Concluding Remarks

The interface charge density matching can be considered as the driving force for the supramolecular self-assembling leading to the mesostructured ICMUV-2 materials described in this work. The possibility of tuning this parameter, which has been accomplished for the first time through the adjustment of the metal mean oxidation state, has allowed us to isolate a wide set of derivatives in the series. The easy elimination of CTA^+ species together with the V:P = 1:1 molar ratio make ICMUV-2 solids adequate pyrolytic precursors of the $(VO)_2P_2O_7$ catalyst.

On the other hand, it seems reasonable to think that the strategy of synthesis reported here will make it possible to readjust previous strategies designed for the isolation of layered and microporous materials to obtain new V−P−O mesoporous solids. Even more, the procedure reported here for the control of the density of charge in the inorganic moiety could be extended to other inorganic systems in which different accessible oxidation states are possible for the metallic centers.

To confirm the suitability of the proposed local structure for ICMUV-2 solids, a more detailed EXAFS characterization is in course in the E.S.R.F.

Acknowledgment. We very much thank the D.G.E.S. of the Spanish Ministerio de Educación y Ciencia (Grant PB95-1094) for financial support of this work. J.E.H. and S.C. thank the A.E.C.I. for doctoral grants. Dr. J. Sanz (ICMM-CSIC, Madrid, Spain) is acknowledged by his collaboration in NMR studies. We very much thank all the referees' comments, which have allowed us to improve our manuscript.

CM9805572